COMMUNICATIONS IN NUMERICAL METHODS IN ENGINEERING
Commun. Numer. Meth. Engng, **14**, 657–670 (1998)

COMPUTING FLUX INTENSITY FACTORS BY A BOUNDARY METHOD FOR ELLIPTIC EQUATIONS WITH SINGULARITIES

M. ARAD,* Z. YOSIBASH, G. BEN-DOR AND A. YAKHOT

Pearlstone Center for Aeronautical Engineering Studies, Department of Mechanical Engineering, Ben-Gurion University of the Negev, Beer-Sheva, Israel

SUMMARY

A simple method for computing the flux intensity factors associated with the asymptotic solution of elliptic equations having a large convergence radius in the vicinity of singular points is presented. The Poisson and Laplace equations over domains containing boundary singularities due to abrupt change of the boundary geometry or boundary conditions are considered. The method is based on approximating the solution by the leading terms of the local symptotic expansion, weakly enforcing boundary conditions by minimization of a norm on the domain boundary in a least-squares sense. The method is applied to the Motz problem, resulting in extremely accurate estimates for the flux intensity factors. It is shown that the method converges exponentially with the number of singular functions and requires a low computational cost. Numerical results to a number of problems concerned with the Poisson equation over an L-shaped domain, and over domains containing multiple singular points, demonstrate accurate estimates for the flux intensity factors.

KEY WORDS flux intensity factors; singularities; multiple singular points; eliptic PDEs

1. INTRODUCTION

Solutions of elliptic linear partial differential equations in two dimensions may contain singular points on boundaries of the solution domain. These points are located at abrupt changes of boundary conditions or re-entrant corners, and first derivatives of the solution tend to infinity as the distance from these points tends to zero. The solution of the Laplace equation $\nabla^2 u = 0$, for example, in the vicinity of a singular point is usually known in the form of an asymptotic expansion with unknown coefficients[1,2],

$$u_{\mathrm{H}}(r,\theta) = \sum_{i=1}^{N}\sum_{s=0}^{S}\sum_{m=0}^{M} A_{ism} r^{\alpha_i+m} \ln^s(r) f_{ism}(\theta) + u_{\mathrm{smooth}} \tag{1}$$

r and θ being the polar co-ordinates of a system located in the singular point, α_i are the eigenvalues (real numbers in the case of the Laplace problem) arranged in ascending order and $f_{ism}(\theta)$ are the eigenfunctions which are analytic. These are uniquely determined by the geometry and the boundary conditions along boundaries intersecting in the singular point. The function u_{smooth}

* Correspondence to: M. Arad, Department of Mechanical Engineering, Ben-Gurion University of the Negev, Beer-Sheva, 84105, Israel.

CCC 1069–8299/98/070657–14$17·50

Received 11 June 1997
Accepted 22 December 1997

belongs to the Sobolev space $H^q(\Omega)$, where q depends on N, and can be made as high as required providing that N is large enough. Except for special cases (when α_i is an integer, or when the multiplicity of an eigenvalue is higher than the multiplicity of the corresponding eigenfunction), $S = 0$. M is either 0 or a positive integer when the boundary near the singular point (at the vertex) is curved. Herein only straight boundaries in the vicinity of the singular point will be addressed, and the special cases where ln (r) terms appear will not be treated; therefore we consider (1) in its simplified form,

$$u_H(r, \theta) = \sum_{i=1}^{N} A_i r^{\alpha_i} f_i(\theta) + u_{\text{smooth}} \tag{2}$$

The eigenpairs $u_i \overset{\text{def}}{=} r^{\alpha_i} f_i(\theta)$ satisfy the governing equation in the domain and the boundary conditions along the parts of the boundary that cause the singularity. Note that, if $\alpha_i < 1$, the corresponding ith term in the expansion (2) for ∇u_H is unbounded as $r \to 0$. We can think of the coefficients A_i of these terms as analogous to the stress intensity factors of elasticity. We generalize this terminology, and refer to all coefficients A_i, whether or not the corresponding terms in (2) are singular, as generalized flux intensity factors (GFIFs). The GFIFs depend on the global problem and are often desirable in many applications.

The computation of GFIFs by standard numerical methods can become very inaccurate, and reasonable engineering accuracy is often impossible or, at least, very costly to obtain. To achieve satisfactory accuracy and convergence rates, special methods taking into account the form of the local solution are often suggested. Based on the mathematical analysis of Li *et al.*,[3] we present in this paper a simple yet efficient numerical method for the computation of GFIFs associated with singular points in a two-dimensional domain, provided that the eigenpairs u_i are known *explicitly*. In Reference 3 a weak formulation based on a bilinear weighted form is considered and the minimum is sought. The present method is a simpler variation of that described in Reference 3, and is also capable of solving the Poisson problem, thus providing the GFIFs with high accuracy. We use the method for two-dimensional Laplace and Poisson equations over domains containing re-entrant corners or abrupt change of boundary conditions. From the engineering point of view, the Laplace and Poisson equations describe several problems of engineering interest such as steady-state heat transfer in an unsmooth domain, fully developed flow in a duct of cross-section containing re-entrant corners, the Saint Venant torsion of a bar having an unsmooth cross-section, the deflection of a membrane with a free half-edge, etc.

The proposed boundary method is based on approximating boundary conditions by the expansion (2) by minimizing a discrete functional. Thus, in the interior of the domain, the solution is approximated by a space which is spanned by the first N leading terms of the expansion (2), i.e. u_i, $i = 1, 2, \ldots, N$. As pointed out, each u_i exactly satisfies the governing equation and the boundary conditions along the boundary causing the singularity. The boundary conditions away from the singular point are imposed in a least-squares sense: we require that the expansion (2) matches the boundary conditions by minimizing a discrete functional. This functional sums the square of the distances between the series and the boundary conditions at a given number of points along the domain boundary. This method has several advantages: (a) the dimension of the problem is reduced by one and, consequently, the computational cost is considerably lower; (b) the generalized flux intensity factors are computed explicitly; (c) the numerical computed GFIFs converge to the exact values exponentially as N is increased.

The formulation of the boundary method is presented in Section 2. Numerical experiments are provided in Sections 3 and 4. We first consider a Laplace equation problem, the Motz problem.[4] This is considered as a classical benchmark problem for testing the various methods proposed in the literature, since exact GFIFs are available in Reference 5 for comparison. GFIFs computed by the boundary method for the Poisson equation over L-shaped domains are also presented, and compared to values computed by the p-version finite element method. We also consider the Poisson equation over a domain containing multiple singular points, where a domain decomposition is required. We conclude with a summary in Section 5.

2. THE NUMERICAL METHOD

Let Ω be a two-dimensional domain bounded by the boundary $\partial\Omega = \cup_i \Gamma_i$, where Γ_i are straight lines called edges. These edges intersect at points called vertices. The two boundaries intersecting in the singular point of interest are denoted by Γ_1 and Γ_2 (see Figure 1). We consider the Poisson equation

$$\nabla^2 u(x, y) = -f(x, y) \quad \text{in} \quad \Omega \tag{3}$$

$$B_i(u) = 0 \quad \text{on} \quad \Gamma_i, \quad i = 1, 2 \tag{4}$$

$$B_i(u) = d_i(x, y) \quad \text{on} \quad \Gamma_i, \quad i \neq 1, 2 \tag{5}$$

where $d_i(x, y)$ are smooth functions on the boundaries, B_i is the trace operator for *Dirichlet boundary conditions*, $\partial/\partial \boldsymbol{n}$ for *Newmann boundary conditions*, where $\boldsymbol{n}$ denotes the outward normal vector to the boundary. The solution to the above problem in the vicinity of a singular point takes the form

$$u = u_{\mathrm{H}} + u_{\mathrm{P}} \tag{6}$$

where u_{H} is given by (2) and u_{P} is a particular solution which satisfies (3) identically.

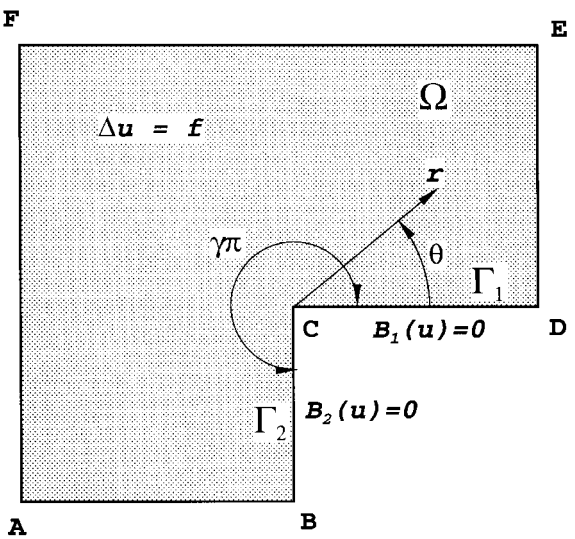

Figure 1. Domain with a re-entrant corner and notation

Herein u is approximated by considering the first N leading terms in the series (2). On $\cup_i \Gamma_i$, $i \neq 1, 2$, we place N_p grid points equally spaced along the boundary, such that for each it is required that (6) satisfies the boundary conditions (5). Non-uniform spacing of the grid points virtually does not change the accuracy of the results. It is essential that N_p is greater than N (for $N_p < N$ one obtains an underdetermined system of equations, whereas for $N_p = N$ one obtains a collocation method). Thus, an overdetermined set of equations is obtained, and the following procedure is applied. We define

$$\mathcal{B} = \sum_{\Gamma_i} \sum_{j=1}^{N_p} \{B_i[u(x_j, y_j)] - d_i(x_j, y_j)\}^2, \quad (x_j, y_j) \in \Gamma_i \tag{7}$$

$\mathcal{B}$ obtains a minimum when the coefficients A_k are the best approximations to the exact values. Thus we have to consider

$$\frac{\partial \mathcal{B}}{\partial A_k} = 0, \quad k = 1, 2, \ldots, N \tag{8}$$

which provides a system of N equations for the N unknown GFIFs.

3. NUMERICAL EXAMPLE: THE MOTZ PROBLEM

We demonstrate the method on the Motz problem,[4] considered as a benchmark problem for testing the various singular methods proposed in the literature; see, for example, References 3 and 6. The geometry, the governing equation and the boundary conditions for the Motz problem as modified by Wait and Mitchell[7] are shown in Figure 2. A singularity arises at $x = y = 0$, where the boundary condition suddenly changes from $u = 0$ to $\partial u/\partial y = 0$. The solution in the vicinity of the singular point is given by

$$u_H = \sum_{k=1}^{\infty} A_k r^{(2k-1)/2} \cos[(2k-1)\theta/2] \tag{9}$$

The above expansion is valid in the entire solution domain. In fact, it has been shown in Reference 5 that the radius of convergence is at least as large as 2 and that the first 20 GFIFs are obtained exactly by a conformal mapping technique.

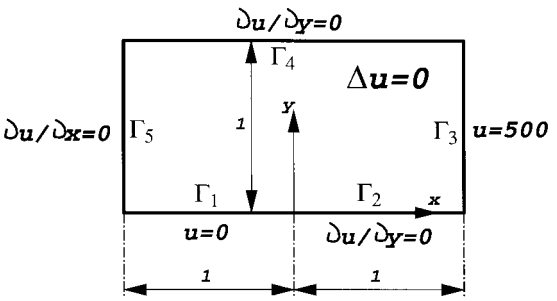

Figure 2. Domain and boundary conditions for the Motz problem

Many special numerical schemes have been proposed for the solution of the Motz problem, including finite difference, global element, boundary element, finite element and others. In what follows we make comparisons with the exact values of Rosser and Papamichael.[5]

The solution u is approximated using the N leading terms of the asymptotic expansion (9), and the derivatives are approximated by

$$\begin{Bmatrix} \dfrac{\partial u}{\partial x} \\ \dfrac{\partial u}{\partial y} \end{Bmatrix} = \frac{1}{2}\sum_{k=1}^{N} A_k(2k-1)r^{(2k-3)/2} \begin{Bmatrix} \cos[(2k-3)\theta/2] \\ -\sin[(2k-3)\theta/2] \end{Bmatrix} \tag{10}$$

At each grid point along the boundary segments Γ_3, Γ_4 and Γ_5 we require that u approximates the boundary conditions. It is essential that the number of grid points N_p is greater than N, obtaining an overdetermined set of equations. Defining

$$\mathcal{B} = \sum_{(x_i,y_i)\in\Gamma_3} [500 - u(x_i, y_i)]^2 + \sum_{(x_i,y_i)\in\Gamma_4} [0 - \partial u(x_i, y_i)/\partial y]^2 + \sum_{(x_i,y_i)\in\Gamma_5} [0 - \partial u(x_i, y_i)/\partial x]^2 \tag{11}$$

$\mathcal{B}$ obtains a minimum when the coefficients A_k are the best approximations to the exact values. Thus we consider

$$\frac{\partial \mathcal{B}}{\partial A_k} = 0, \quad k = 1, 2, \ldots, N \tag{12}$$

which produces a system of N linear algebraic equations presented in a matrix form by

$$[K]\{A\} = \{r\} \tag{13}$$

The matrix $[K]$ is a symmetric matrix which is fully populated. As N_p is increased, for a given N, the condition number of the matrix $[K]$ is improved. In Table I we show the effect of N_p on the calculated values of A_1, A_5, A_{10}, A_{15} and A_{20} obtained with $N = 40$. One notices that the values of the GFIFs converge with N_p and that highly accurate estimates are obtained at least for the

Table I. Convergence of the GFIFs with N_p ($N = 40$)

N_p	A_1	A_5	A_{10}	A_{15}	A_{20}	Cond.
41	401·1624537506	1·4402727165	0·0153843744	0·0002715122	−0·0000052957	$4{\cdot}95_{10}7$
61	401·1624537453	1·4402727170	0·0153843745	0·0002715122	−0·0000052958	$8{\cdot}63_{10}6$
81	401·1624537452	1·4402727170	0·0153843745	0·0002715122	−0·0000052958	$7{\cdot}76_{10}6$
101	401·1624537452	1·4402727170	0·0153843745	0·0002715122	−0·0000052958	$7{\cdot}27_{10}6$
121	401·1624537452	1·4402727170	0·0153843745	0·0002715122	−0·0000052958	$6{\cdot}94_{10}6$
141	401·1624537452	1·4402727170	0·0153843745	0·0002715122	−0·0000052958	$6{\cdot}71_{10}6$
161	401·1624537452	1·4402727170	0·0153843745	0·0002715122	−0·0000052958	$6{\cdot}54_{10}6$
Exact	401·1624537452	1·4402727170	0·0153843745	0·0002715122	−0·000005295	

Table II. Convergence of the solution as N increases ($N_p = 161$)

N	A_1	A_5	A_{10}	A_{15}	A_{20}	Cond.
20	401·1624601517	1·4402703003	0·0153455497	0·0002398586	−0·0000061606	$4{\cdot}07_{10}3$
25	401·1624538791	1·4402728589	0·0153831210	0·0002687029	−0·0000058721	$2{\cdot}61_{10}4$
30	401·1624537608	1·4402727275	0·0153843513	0·0002713616	−0·0000053706	$1{\cdot}48_{10}5$
35	401·1624537452	1·4402727161	0·0153843744	0·0002715173	−0·0000052845	$9{\cdot}90_{10}5$
40	401·1624537452	1·4402727170	0·0153843745	0·0002715122	−0·0000052958	$6{\cdot}54_{10}6$
45	401·1624537452	1·4402727170	0·0153843745	0·0002715122	−0·0000052958	$3{\cdot}84_{10}7$
50	401·1624537452	1·4402727170	0·0153843745	0·0002715122	−0·0000052957	$2{\cdot}18_{10}8$
Exact	401·1624537452	1·4402727170	0·0153843745	0·0002715122	−0·000005295	

20 leading coefficients. In the last column we introduce the condition number associated with the matrix $[K]$,

$$\text{cond} = \left(\frac{\lambda_{\max}}{\lambda_{\min}}\right)^{1/2} \tag{14}$$

where $\lambda_{\max}$ and $\lambda_{\min}$ are the largest and smallest eigenvalues of $[K]$, respectively. One may see that for $N_p > 2N$ the results are practically independent of N_p.

In Table II we show the convergence of the GFIFs as N increases with $N_p = 161$. One notices that the values of the singular coefficients converge rapidly with N. It is visible that there is a loss of stability as N increases (i.e. the condition number becomes larger). A similar loss of stability was observed by Li *et al.*[3] and Georgiou *et al.*[6] The exponential convergence rate of the method is illustrated in Figure 3, where the absolute error of A_1 as a function of $N(N_p = 161)$ is plotted. The first 20 coefficients obtained with $N = 40$ and $N_p = 161$ are as accurate as the exact values presented in Reference 5. The present method yields accurate GFIFs and requires a smaller computational effort when compared to other methods given in References 3 and 5.

3.1. Motz non-symmetric problem

The method was checked on a variation of the Motz problem with a larger and non-symmetric domain shown in Figure 4. 'Motz boundary conditions' are kept on the five segments of the boundary. Taking $N = 20$ and $N_p = 31$ the first six GFIFs obtained are: $A_1 = 169{\cdot}8046$, $A_2 = 36{\cdot}9230$, $A_3 = 7{\cdot}0542$, $A_4 = -3{\cdot}6406$, $A_5 = 0{\cdot}4543$ and $A_6 = 0{\cdot}0494$. In order to check the accuracy of these GFIFs, the p-version of the finite element method was used to compute these GFIFs over the mesh shown in Figure 5. The p-level over the elements has been increased from 1 to 8, obtaining an estimated relative error in energy norm at $p = 8$ of less than 0·2 per cent with 1839 degrees of freedom (see Reference 8 for details on the estimation of the error in energy norm). Using the finite element commercial code Stress Check* the following GFIFs are obtained: $A_1 = 169{\cdot}799$, $A_2 = 36{\cdot}923$, $A_3 = 7{\cdot}054$, $A_4 = -3{\cdot}642$, $A_5 = 0{\cdot}454$ and $A_6 = 0{\cdot}0495$. The results, obtained by different methods, agree with each other very well, ensuring their accuracy. The question of the accuracy of the results obtained using the *local* expansion to approximate the exact solution *away* from the singular point is addressed in the following Section.

*Stress Check is the Trade Mark of Engineering Software Research and Development, Inc., 7750 Clayton Road, Suite 204, St. Louis, MO 63117, U.S.A.

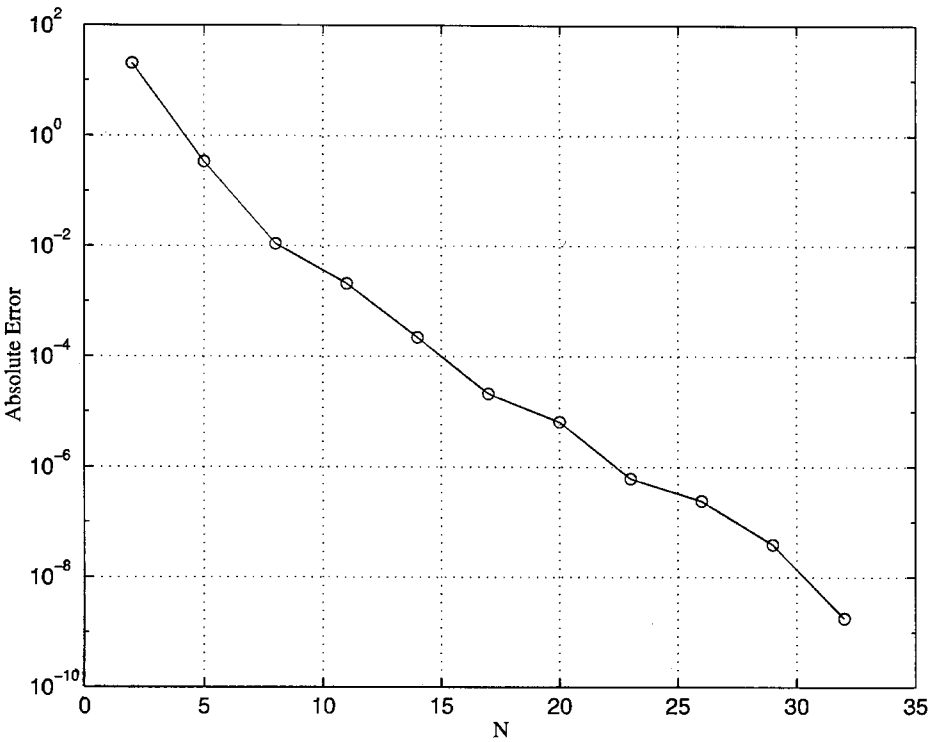

Figure 3. Absolute error of A_1 as a function of N ($N_{p=161}$)

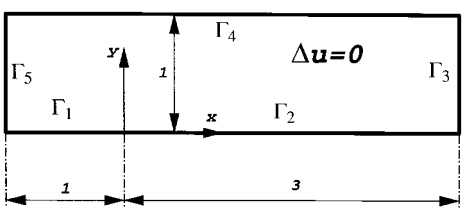

Figure 4. Domain and boundary conditions for the non-symmetric Motz problem

4. NUMERICAL EXAMPLE: POISSON EQUATION OVER AN L-SHAPED DOMAIN

In this Section the Poisson equation $\nabla^2 u = -1$ over the domain illustrated in Figure 6 is considered, with homogeneous Dirichlet boundary conditions applied over the whole boundary. The exact solution to this problem in the vicinity of the singular point consists of two parts:

$$u_{\mathrm{H}}(r, \theta) = \sum_{k=1}^{\infty} A_k r^{2k/3} \sin(2k\theta/3) \tag{15}$$

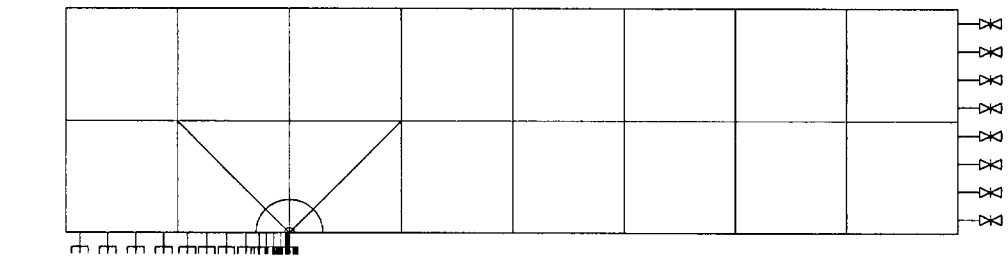

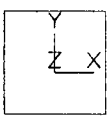

Figure 5. Finite element mesh for the non-symmetric Motz problem

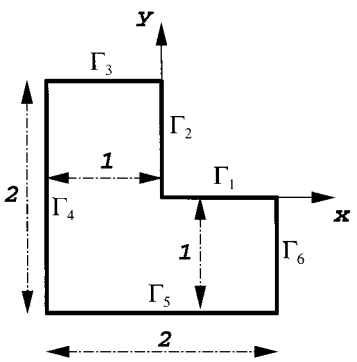

Figure 6. Solution domain for Poisson equation

and[9]

$$u_{\mathrm{P}}(r,\theta) = \frac{-r^2}{6\pi}\left[\frac{3\pi}{2} + 2\ \ln(r)\sin(2\theta) + \left(2\theta - \frac{3}{2\pi}\right)\cos(2\theta)\right] \tag{16}$$

$u = u_{\mathrm{H}} + u_{\mathrm{P}}$ represents in engineering practice the Prantl stress potential (see, for example, Reference 10, Chapter 35) from which the stress tensor to the Saint Venant torsion of a straight bar can be obtained. This problem, for example, is of technical importance in fracture mechanics, and the 'stress intensity factor' defined by $\frac{2}{3}A_1$ is often sought.

Exact GFIFs to the problem of interest are unavailable. However, numerical tests using multigrid methods are reported in Reference 11, where $A_1 = 0{\cdot}40192487$ is accurate to the fourth

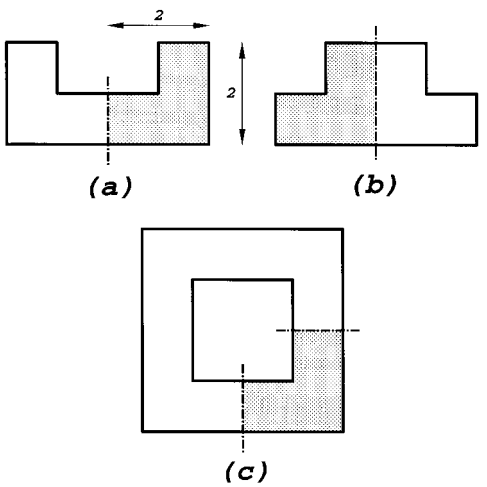

Figure 7. Cross-sections of domains over which Poisson equation is applied

significant digit, and $A_2 \approx 0$. It is known that all the even terms in (15) vanish, so we may expect that the computation will yield $A_2 = A_4 = \cdots = 0$.

Again, the homogeneous part of the solution is approximated by the $N = 10$ leading terms of the symptotic series (15), and we assign $N_P = 61$ grid points along the boundary segments $\Gamma_3 - \Gamma_6$. The results obtained are $A_1 = 0{\cdot}401920085$ and $A_2 = 10^{-17}$, which agree very well with Reference 11.

We also consider a number of problems associated with the torsion of a long rod having cross-sections shown in Figure 7. All cross-sections are composed of identical L-shaped blocks. Each of the cross-sections (a) and (b) contains two such blocks and has one axis of symmetry, whereas cross-section (c) contains four L-shaped blocks and has two axes of symmetry. In each of the cases (a)–(c) we exploit the geometrical symmetry and consider only one shaded L-shaped block, while imposing appropriate symmetry boundary conditions on the axes of symmetry. Thus, only one singular point is considered in each case. For these cases the derivatives $\partial u_H/\partial x + \partial u_P/\partial x$ and $\partial u_H/\partial y + \partial u_P/\partial y$ are computed from (15) and (16), respectively.

The first GFIFs for the problems in Figure 7 as obtained with $N = 10$ and $N_P = 61$ are summarized in Table III. We compare our results to those reported in Reference 12 (in which a low number of degrees of freedom has been used ($N = 5$) and 31 nodal points are used at the DtN boundary) and also with the results computed using finite element analysis over the mesh shown in Figure 8, having 742 DOF at $p = 8$ and an estimated relative error in energy norm of 0·13 per cent. Again the finite element analysis was performed using Stress Check™.

Table III. Values of first GFIF for problems shown in Figure 6

Case no.	Reference 12	FE	Present method
(a)	0·4162	0·4102	0·4101
(b)	0·5527	0·5447	0·5471
(c)	0·4245	0·4185	0·4183

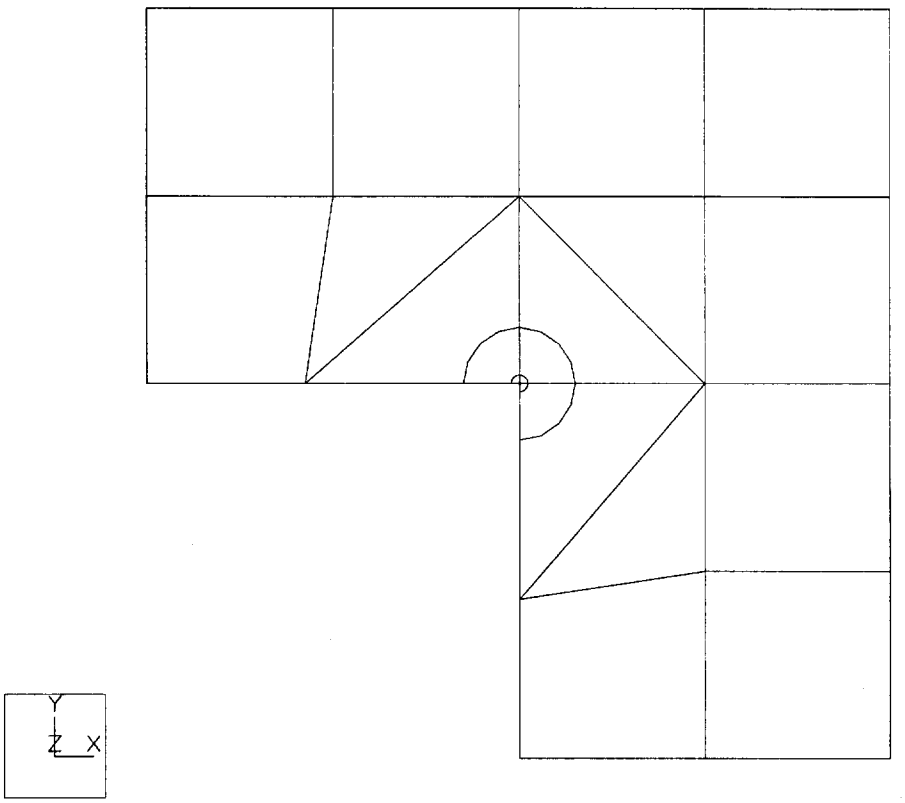

Figure 8. Finite element mesh for Poisson problems shown in Figure 7

4.1. Large L-shaped domains

Herein we address the accuracy of the proposed method when applied over large domains. This is of particular interest since it is known that series (2) is an asymptotic series, i.e. fewer terms are needed as one approaches the singular point. We consider herein an L-shaped domain which is ten times larger than the domain shown in Figure 6. Again, the homogeneous part of the solution is approximated by the $N = 10$ leading terms of the asymptotic series (15), and we assign $N_P = 61$ grid points along the boundary segments. The results obtained are $A_1 = 8{\cdot}65912216$ and $A_2 = -10^{16}$. The obtained GFIFs are compared to the ones extracted using the finite element method, which are $A_1 = 8{\cdot}6682$ and $A_2 = 0$. this comparison shows excellent agreement.

Although the GFIFs are associated with the close vicinity of the singular point, we show that when the series satisfies the boundary conditions away from the singularity we still obtain accurate estimation of GFIFs. An explanation of this situation follows. Let us consider the Poisson equation over a domain which is M times larger than a 'unity' domain in Figure 6. The solution over the large domain will be denoted by $u^{\{M\}}$ and satisfies the equation

$$\nabla^2 u^{\{M\}} = u^{\{M\}}_{xx} + u^{\{M\}}_{yy} = -\mu \tag{17}$$

where μ is a constant. For example, the aforementioned problem had $M = 10$. We define new co-ordinates

$$X = \frac{x}{M}, \qquad Y = \frac{y}{M} \tag{18}$$

consequently, the polar co-ordinates R, Θ are associated with r, θ by $R = r/M$, $\Theta = \theta$. The Poisson equation (17) in the new co-ordinate system takes the form

$$u^{\{M\}}_{XX} + u^{\{M\}}_{YY} = -M^2\mu \tag{19}$$

which is a Poisson equation over the 'unity' domain. This explains the fact that the method is suitable to any bounded domain.

It is also interesting to note that one can obtain immediately the GFIF to any domain which is larger by a factor M, having in hand the GFIF to the 'unity' domain when μ is a constant and the boundary conditions are homogeneous. Comparing (17) and (19), the following connection is obtained:

$$u^{\{M\}}(r, \theta) = M^2 u^{\{1\}}(R, \Theta) \Rightarrow A_1^{\{M\}} r^{2/3} f_1(\theta) = M^2 A_1^{\{1\}} \left(\frac{r}{M}\right)^{2/3} f_1(\theta)$$

which becomes

$$A_1^{\{M\}} = M^{4/3} A_1^{\{1\}}$$

Indeed, the obtained A_1 computed in this sub-section is associated with the A_1 computed over the 'unity' domain at the beginning of Section 4:

$$A_1^{\{10\}} = 10^{4/3} \times 0{\cdot}40192085 = 8{\cdot}65912216$$

which agrees with the numerical value above.

Convergence of solutions using this method is ensured only when there are no additional points of singularity in the domain. In the case of a domain which has more than one singular point, it is necessary to subdivide it into several subdomains, as explained in the next subsection.

4.2. Subdivision of the Domain

For problems with material interfaces or multiple singularities, it is not possible to find a single expansion valid in the entire domain. It is therefore necessary to subdivide it into several subdomains and use different expansions in each of them. A solution is then obtained by approximating both the boundary conditions and the continuity conditions across the interior artificial interface. We note that for a good subdivision only a few terms are needed in each subdomain to achieve an accurate approximation. Moreover, the numerical stability is greatly improved and the matrix $[K]$ has many zero entries. To demonstrate the subdivision technique, we consider the Poisson equation $\nabla^2 u = -1$ over the domain shown in Figure 9 with homogeneous Dirichlet boundary conditions applied over the entire boundary. Due to the two singular points, two subdomains, Ω_1 and Ω_2, are defined. In each subdomain we consider a series of the form (15) and (16). These series have to satisfy the continuity conditions across the interface at selected grid points. These requirements may not be fulfilled exactly but only in a least-squares form, enabling

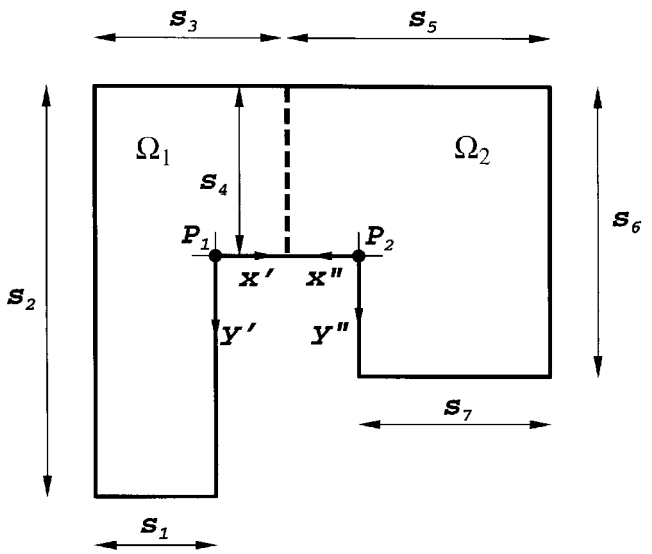

Figure 9. Domain with two singular points and notation

a flexibility between the approximations which improves the accuracy. Continuity across the artificial boundary is required on the solution u as well as on the normal derivative of u. These continuity conditions were applied to be consistent with the outer boundary conditions $\partial\Omega$. This also simplifies the programming difficulties. Similar continuity conditions were proposed by Li *et al.*[3]

For a domain with $S_1 = 2$, $S_2 = 8$, $S_3 = 3$, $S_4 = 4$, $S_5 = 4$, $S_6 = 6$, $S_7 = 3$, we chose $N_{(\Omega_1)} = 10$, $N_{(\Omega_2)} = 10$ and a grid size on all the boundaries (the distance between adjacent grid points) $h = 1$. The first two computed GFIFs for the singular point P_1 (in the domain Ω_1) and P_2 (in Ω_2) are:

$$\text{at } P_1: \quad A_1 = 1{\cdot}6042, \quad A_2 = 0{\cdot}3533$$
$$\text{at } P_2: \quad A_1 = 2{\cdot}0403, \quad A_2 = 0{\cdot}2332$$

The condition number associated with the problem is $1{\cdot}4354 \times 10^4$.

Since neither analytic nor numerical approximations to this problem are available, we solve the same problem using finite elements (Stress Check™) over the mesh shown in Figure 10. At $p = 8$, with 2361 DOF, the relative error in energy norm is 0·08 per cent, and the first two GFIFs are:

$$\text{at } P_1: \quad A_1 = 1{\cdot}6013, \quad A_2 = 0{\cdot}3504$$
$$\text{at } P_2: \quad A_1 = 2{\cdot}0333, \quad A_2 = 0{\cdot}2329$$

As may be noted, the first two GFIFs obtained by the two different numerical techniques are very similar, confirming the accuracy of the presented method.

5. CONCLUSIONS

A simple boundary method has been presented for computing the generalized flux intensity factors associated with the singular solution of two-dimensional elliptic boundary value

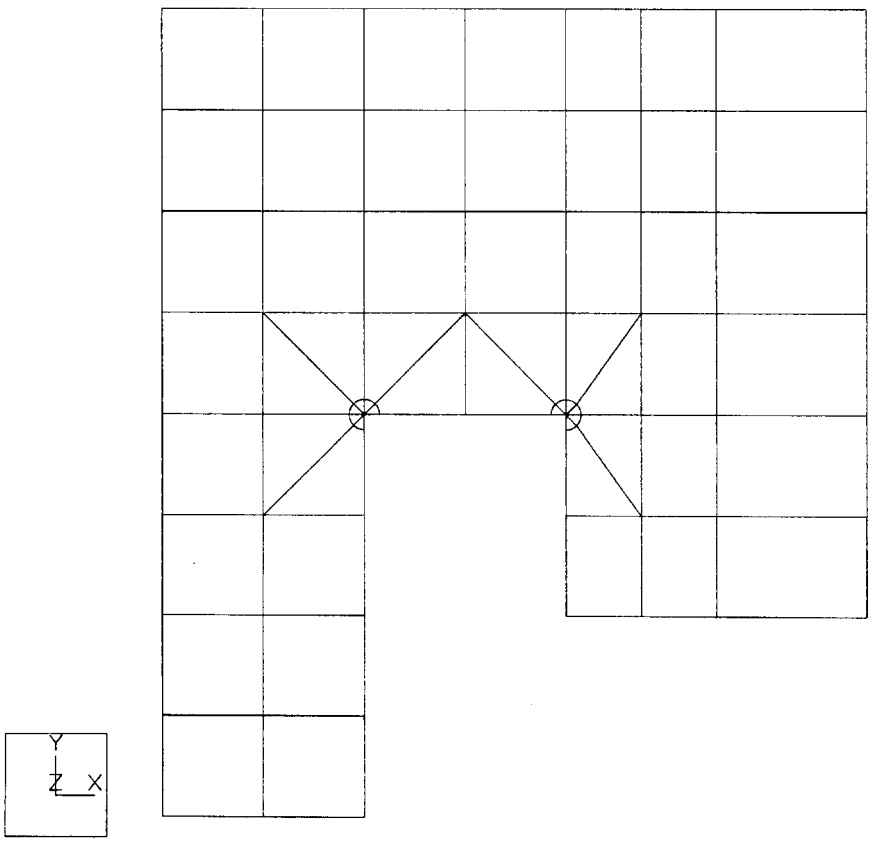

Figure 10. Finite element mesh for Poisson problem containing multiple singular points as shown in Figure 9

problems arising from abrupt changes in the boundary conditions or in the direction of the boundary. The method has several advantages: (a) the dimension of the problem is reduced by one and, consequently, the computational cost is considerably lower; (b) the generalized flux intensity factors are computed explicitly; (c) the numerical computed GFIFs converge to the exact values exponentially as N is increased.

The method may be extended to elliptic problems involving other types of singularities, such as those caused by an interface between two different elastic materials, for example, provided that the form of the asymptotic series for the solution in the vicinity of the singular point is known.

REFERENCES

1. V. A. Kondratiev, 'Boundary value problems for elliptic equations in domains with conical or angular points', *Trans. Moscow Math. Soc.*, **16**, 227–313 (1967).
2. P. Grisvard, *Elliptic Problems in Nonsmooth Domains*, Pitman Publishing, England, 1985.
3. Z-C. Li, R. Mathon and P. Sermer, 'Boundary methods for solving elliptic problems with singularities and interfaces', *SIAM J. Numer. Anal.*, **24**(3), 487–498 (1987).
4. H. Motz, 'The treatment of singularities of partial differential equations by relaxation methods', *Q. Appl. Math.*, **4**, 371 (1946).

5. J. B. Rosser and N. Papamichael, 'A power series solution of a harmonic mixed boundary value problem', *MRC Technical Summary, Rept. 1405*, University of Wisconsin, 1975.
6. G. C. Georgiou, L. G. Olson and Y. S. Smyrlis, 'A singular function boundary integral method for the Laplace equation', *Commun. Numer. Methods Eng.*, **12**, 127–134 (1996).
7. R. Wait and A. R. Mitchell, 'Corner singularities in elliptic problems by finite element methods', *Comput. Phys.*, **8**, 45 (1971).
8. B. A. Szabó and I. Babuška, *Finite Element Analysis*, Wiley, New York, 1991.
9. H. K. Moffatt and B. R. Duffy, 'Local similarity solutions and their limitations', *Fluid Mech.*, **96**, 299–313 (1980).
10. I. S. Sokolnikoff, *Mathematical Theory of Elasticity*, McGraw-Hill, New York 1956.
11. C. Susanne Brenner, 'Multigrid methods for the computation of singular solutions and stress intensity factors. I: Corner singularities', Preprint submitted to *Math. Comput.*, 1996.
12. D. Givoli and L. Rivkin, 'The DtN finite element method for elastic domains with cracks and re-entrant corners', *Comput. Struct.*, **49**, 633–642 (1993).

